

Application of the full factorial design to modelling of Al₂O₃/SiC particle reinforced al-matrix composites

Necat Altinkok*

*Department of Machine and Metal Technologies Sakarya University,
Hendek Vocational School, Hendek, Sakarya, Republic of Turkey*

(Received November 23, 2015, Revised August 04, 2016, Accepted August 17, 2016)

Abstract. Al₂O₃/SiC particulate reinforced (Metal Matrix Composites) MMCs which were produced by using stir casting process, bending strength and hardening behaviour were obtained using an analysis of variance (ANOVA) technique that uses full factorial design. Factor variables and their ranges were: particle size 2-60 μm; the stirring speed 450 rpm, 500 rpm and the stirring temperature 620°C, 650°C. An empirical equation was derived from test results to describe the relationship between the test parameters. This model for the tensile strength of the hybrid composite materials with R^2 adj = 80% for the bending strength R^2 adj = 89% were generated from the data. The regression coefficients of this model quantify the tensile strength and bending strengths of the effects of each of the factors. The interactions of all three factors do not present significant percentage contributions on the tensile strength and bending strengths of hybrid composite materials. Analysis of the residuals versus was predicted the tensile strength and bending strengths show a normalized distribution and thereby confirms the suitability of this model. Particle size was found to have the strongest influence on the tensile strength and bending strength.

Keywords: hybrid particulate reinforced composites; the tensile strength; bending strengths; hardness; porosity; full factorial design; analysis of variance (ANOVA)

1. Introduction

The demand of ceramic particle reinforced MMCs for lightweight materials having high strength, high stiffness, wear resistance and tailor able thermal expansion characteristics have taken much interest in the development of the fabrication processes (Chou *et al.* 2006, Lloyd and Brotzen 1999, Sato and Mehrabian 1976). The perfect mechanical properties of these materials and the relatively low production cost make them very attractive for various applications in automotive industry. There are several fabrication techniques to obtain MMCs. Many techniques were developed for producing particulate reinforced MMCs, such as powder metallurgy (Han *et al.* 1995), in situ (Caracostas *et al.* 1997) squeeze casting (Kong *et al.* 1996), stir casting (Gopalakrishnan and Murugan 2012) and liquid metal infiltration. From all the above five methods, stir casting technique is the simplest and the most economical process for fabricating particulate reinforced MMCs (Gopalakrishnan and Murugan 2012).

*Corresponding author, Associate Professor, E-mail: altinkok@sakarya.edu.tr

^a Ph.D., E-mail: altinkok@sakarya.edu.tr

Several different methods are being searched in case of improving suitability at the interface, squeeze-casting work method of these is the most appropriate, since the time of the intercourse between the consolidation and the melt is short, thus interface reaction is limited and wettability raised (Gupta *et al.* 1991). The hardening processes in MMCs are limited. Frankly, this kind of information could be much rewarding in case of improving the features of MMCs in the actual production work. The structure of hardening and the features of Al₂O₃/SiCp A332 composite are studied. The mechanical properties of the composites are influenced significantly by the quantity and mode of distribution of the reinforcements and by the nature of the interfaces between the reinforcements and the matrix (Gupta *et al.* 1991, Peters *et al.* 2010). MMCs in general consist of at least two components, namely matrix and the reinforcement. The matrix is usually an alloy, and the reinforcement is usually a ceramic. The aim involved in designing MMC materials is to combine the desirable attributes of metals and ceramics (Ezatpour *et al.* 2014).

Fabrication methods of the composites can be categorized into three processes: solid-state methods, semi-solid-state methods and liquid-state methods. Stir casting is a liquid-state method of composite materials fabrication, in which a dispersed phase (ceramic particles or short fibers) is mixed with a molten matrix metal by means of the mechanical stirring. Compared with solid-state methods, melt processing which involves stirring of ceramic particles into melt, has some important advantages: better matrix-particle bonding, easier control of matrix structure, simplicity, low cost of processing and nearer net shape and the wide selection of Materials for this fabrication method (Kok 2005). Depending on the temperature at which the particles are introduced into the melt, there are two types of melting methods for making composites. In the liquid metallurgy process the particles are incorporated above the liquid temperature of the molten alloy, while in compocasting method the particles are incorporated into the semi-solid slurry (Sajjadi *et al.* 2012).

Research has been conducted in recent years on production of MMCs by stir casting technique. But very little research work has been done on stirring speed and stirring time required for uniform distribution of particle in the matrix. Hashim *et al.* (1999, 2002) attempted some research on stir casting technique. (Naher *et al.* 2003) studied the effect of stirring speed on uniform distribution of particle by simulation. They have conducted experiments on fluids with similar characteristics of liquid and semisolid aluminium. SiC reinforcement particulate similar to that used in aluminium MMCs was used in the simulation fluid mixtures. But an experimental investigation on this problem is very little. The main objective of this work is to reveal the influence of stirring speed and stirring time on the uniform distribution of SiC particle in the aluminium alloy matrix (Prabu *et al.* 2006, Roy 2001).

Most of the investigations employed Taguchi techniques, such as orthogonal arrays and S/N ratio analysis in order to find out the optimal values of cutting parameters that minimize the response variable. Taguchi methodology allows obtaining results using fewer experimental runs than other techniques. The results obtained may be not optimal, but when these results are implemented, process is improved. Therefore, less money and time are spent when Taguchi techniques are employed. The quality engineering method known as Taguchi method or Taguchi approach is an experimental strategy in which a modified and standardized form of Design of Experiment (DOE) is used. Taguchi created a number of special orthogonal arrays and to analyse the results he introduced the use of the signal-to-noise ratio (S/N ratio) to assure a design that is immune to the influence of uncontrollable factors. Taguchi analysed results based in the deviation from the target. Consequently, selection of the design condition which leads to improved quality is allowed (Roy 2001, Carmita 2013).

Design of experiment (DOE) technique is one of the most significant statistical techniques to

study the effects of multiple control factors (process variables) on responses. It involves a series of steps that should be followed in a certain sequence for the experiment to yield results that can be deciphered for the better understanding of the process. As per DOE, experiments require a certain number of combinations of control factors at different levels such that the responses can be tested for characterizing the process. A major step in the DOE is to determine of the combination of factors and levels which will provide the desired information. The full factorial plan of experiment takes into account all possible combination of control factors to yield the responses. When the number of control factors is a few then full factorial plan of experiment is desirable. The DOE technique has been successfully used by researchers to study the tribological behaviour of composites (Fisher 1961, Anand *et al.* 2013).

Tests, based on the design of experiments (DOE) technique, were conducted to systematically record the influence of precipitation hardening parameters on the fatigue strength of AA 6061-SiCp composite (Ceschini *et al.* 2006). The plan of full factorial experiment on abrasive wear properties of in-situ Al-4.5%Cu/TiC MMCs well exhibited the interaction effects of the control factors on the responses success has weight loss and coefficient of friction. ANOVA of weight loss and coefficient of friction helped in building regression equations based on the significance of control factors and interactions (Anand *et al.* 2013, Elayaperumal and Issac 2013).

A full factorial investigation, in which all possible combinations of the values of the experimental variables (the factors) are evaluated, provides a thorough method for determining all the interactions within the range of conditions of interest. This approach can also be used to generate an empirical expression for the response in terms of the variables studied (Trezona *et al.* 2000).

(Radhika *et al.* 2011) found taguchi technique as a valuable technique to deal with responses influenced by multivariable. It is formulated for process optimization and detection of optimal combination of the parameters for a given response. This method significantly reduces the number of trials that are required to model the response function compared with the full factorial design of experiments. The most important benefit of this technique is to find out the possible interaction between the factors.

The experiment is planned in such a way to estimate simultaneously two or more factors which possess their ability to affect the resultant average or variability of particular product or process characteristics. To accomplish this in a valuable and statistically proper method, levels of the factors are varied in a strategic manner. The results of the particular test combinations are observed and the complete set of results are analysed to determine the preferred level of the various influencing factors whether increases or decreases of those levels will potentially lead to further enhancement Ross (1996).

In this study, input parameters of particle size was optimized to determine the tensile strength and bending strength for Al₂O₃/SiC particles reinforced hybrid composites by using Taguchi's full factorial experimental design methodology.

2. Experimental

Al₂O₃/SiC particles reinforced metal matrix composites (MMCs) are produced by stir casting. The mechanical and physical properties of Al₂O₃ and SiCp are given in Table 1. The chemical composition of the A332 Al-Si alloy is shown in Table 2. By starting investigation, dual ceramic mixture was made ready by using chemical route and then was added A332 composite in melted

Table 1 The mechanical and physical properties of Al₂O₃, SiC_p and matrix materials

| Material | Density values (g/cm ³) | Diameter (μm) | Modulus (GPa) | HV |
|--|-------------------------------------|------------------|---------------|------|
| A332 Al-Si alloy | 2,7 | - | 91 | 81 |
| Al ₂ O ₃ | 2,9 | ~3 | 308 | 1998 |
| SiC _p | 3,2 | 2-10-20-38-45-53 | 409 | 2800 |
| Al ₂ O ₃ /SiC _p | 3,05 | 2-10-20-38-45-53 | 358,5 | 2000 |

Table 2 Chemical analysis of the A332 Al-Si alloy (Azmah *et al.* 2011)

| Element | Si | Cu | Mg | Fe | Ni | Zn | Mn | Pb | Ti | Sn | Al |
|---------|----------|---------|---------|-----|----|----|-----|-----|-----|-----|-----------|
| wt% | 8,5-10,5 | 2,0-4,0 | 0,5-1,5 | 1,2 | 1 | 1 | 0,5 | 0,2 | 0,2 | 0,1 | Remainder |

condition by using stir casting procedure. Al₂O₃ was chemically generated from aluminium sulphate while SiC particles were commercially procurement. Al₂O₃/SiC_p combination was made ready and heated in the furnace by using melting pot. Then Al₂O₃/SiC particle ceramic cake was produced. This cake was milled in case of adjusting particle size before stir casting. This dual ceramic powder obtained with various SiC particle sizes was included into liquid matrix composite. Bending force and hardness resistance of Al₂O₃/SiC_p strengthened MMCs and reinforced particle size influence on the tensile stress are studied. This mechanical study showed that the tensile strength, bending and hardness resistance of 10 vol.% Al₂O₃/SiC_p dual ceramic powder composites declines while strength of SiC particle size raises. In the hybrid MMCs, both the reinforcing materials, Al₂O₃ and SiC_p, are used at different sizes. The matrix materials yield strength was measured as 224 MPa. The ultimate the tensile strength of the same material is 229 MPa and the bending strength is 315.3 MPa.

2.1 The mechanical tests and microstructure analysis

The mechanical tests of the cast composites carried out by a Dartec Universal Testing Machine (Dartec, Stourbridge, West Midlands, DY9 8SH, and UK) type testing machine at room temperature with 1m/s speed under. Test samples were prepared according to ASTM B-312 standard. To study on particles distribution, Optical microscope (Olympus BH2-UMA) was utilized. For examination of polish surfaces, with addition of energy-dispersive-spectroscopy (EDS) analysis at low voltage of 5kV, SEM (Jeol 5600): by Jeol Ltd., Tokyo, Japan was used. The evaluation of intensity values was applied based on Archimend Principles. The porosity of composites was calculated as $1 - \rho_m / \rho_{th}$ where ρ_m and ρ_{th} were the measured and theoretical density values respectively. Brinell hardening values of Al₂O₃/SiC particle aided MMCs materials were obtained by using Wolpert Testor HT1a type machine with 187.5 kg load and 2,5 mm dimensional steel ball at the end of 30 seconds.

In Fig. 1 SEM images of the produced ceramic preform are shown. Before obtaining stir casting, this ceramic cake is granulated for calibration of particles size. With different SiC particle dimensions, those dual ceramic powders are mixed with liquid matrix composite. The effect of size of reinforcing particle on the tensile strength, resistance of bending and strength of hardness for MMCs reinforced by Al₂O₃/SiC_p are studied (Fig. 2).

At the end of the microscopic experiments, as shown in Fig. 2, Al₂O₃/SiC particles are well

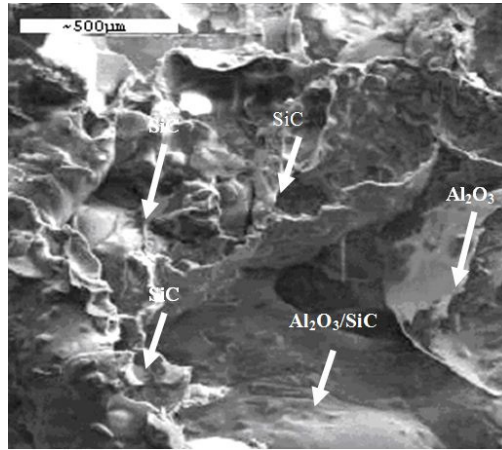
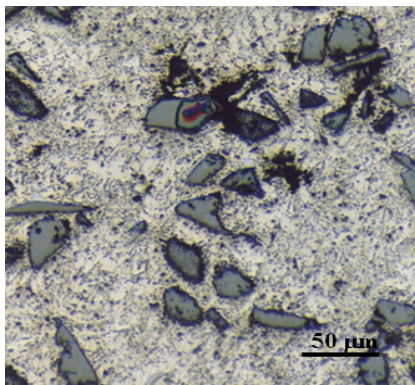
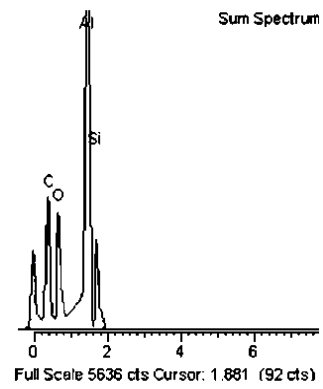


Fig. 1 SEM images of porous ceramic preform Al₂O₃/SiC particle ceramic cake

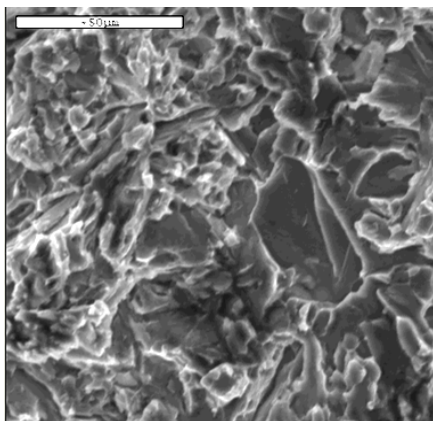


(a) Polish surface of optical micrograph

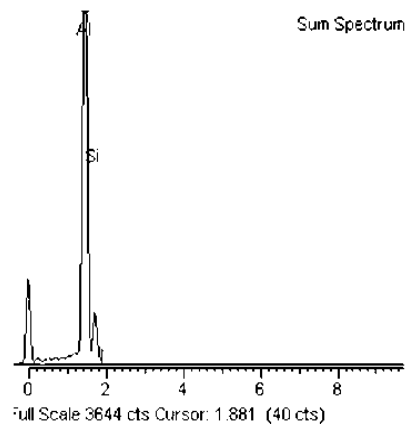


(b) EDS analysis

Fig. 2 SiC with Al₂O₃ reinforced MMC



(a) Fracture surface of SEM micrograph



(b) EDS analysis

Fig. 3 A332 matrix alloy

dispersed in the matrix and fully wetted by molten aluminium. Those particles are available to enhanced mechanical characteristics. Silicon and magnesium in melted liquid aluminium enhanced wettability of matrix and supported the particles incorporation. An optical microstructure belong to stir cast composite is shown in Fig. 2(a). This figure shows that big $\text{Al}_2\text{O}_3/\text{SiC}$ particles along with small ones which reinforced MMC are successfully produced. SEM and polish surface optical views with EDS analysis of matrix alloy are illustrated in Fig. 2(b) whereas, Oxygen and carbon peak from analysis of EDS approves that alumina and SiC particles are present within the composites is shown in Fig. 3(a)-(b), those elements do not exist to show Al-Si-Mg matrix alloy.

Composites reinforcement amount is provided as $\text{Al}_2\text{O}_3/\text{SiCp}$ with 10% vol., density measurement and porosity have been changed considering reinforcement size. The composites density values have been reduced because of porous among the gathered $\text{Al}_2\text{O}_3/\text{SiC}$ particles and the porosity in matrix (Gui *et al.* 2000). The decreases on the particle dimensions make the tensile, hardness resistance of MMCs and bending strength increased because of reduced particle sizes and increased particles in numbers in a unit volume. The composites fracture surfaces, which have been used in the tensile strength study, is given in SEM (scanning Electron Microscope) image in Fig. 4(a), oxygen and carbon peak from analysis of elemental diffraction scanning (EDS) approve that alumina and SiC particles are available within the composites. Sliding type plastic deformations and dimples have been seen on the fraction surface. But then, some cracked points have monitored on $\text{Al}_2\text{O}_3/\text{SiC}$ particles in some regions. The study result showed that the crack on the particles gets clearer while the reinforcement particle sizes decrease.

The MMCs microstructure used in the studies has been changed depending on casting cooling rate. Those cooling rate influences the distribution of $\text{Al}_2\text{O}_3/\text{SiC}$ particles in the casting. This effect becomes important in the case of composite, because $\text{Al}_2\text{O}_3/\text{SiC}$ particle distribution is affected by growing aluminium are pushed by the leading edges of growing aluminium dendrites. Since the cooling speed affects the particles distribution in casting process, hardness resistance has been affected. Increased cooling has caused the formation of small dendrites and for this reason; the particles have been very uniformly distributed. In addition to this homogeneity distribution and reduction of particle size, the tensile, bending strength and hardness resistance of MMCs have been increased. These properties have been played important role on mechanical properties of composite. Srivatsan (1996) has been presented similar results.

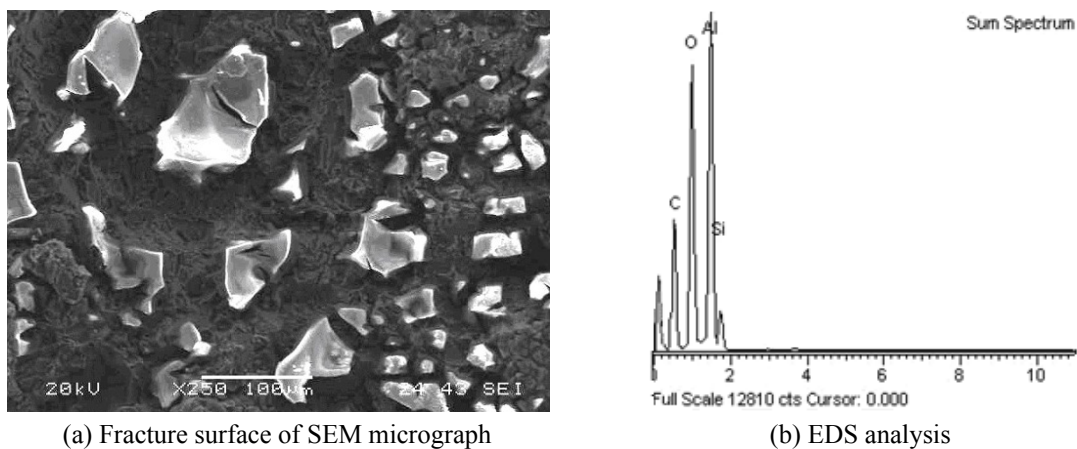


Fig. 4 SiC with Al_2O_3 reinforced MMC

By the decreasing of reinforced particle size for Al₂O₃/SiC particle composite, the amount of porosity has been increased. Since decreasing particle size and increasing particles in numbers in a unit volume, the larger surface area has been taken shape. Accordingly, this feature increases the surface energy of particles. Decreasing particle size is the reason for increasing amount of porosity. (Swamy *et al.* 2011) have been presented similar results. Additionally, during producing composite material process, the porosities which have been existed with particle reinforcement

Table 3 Control factors and theirs levels for full factorial design

| Control factors | Level | | | | | | | | Units |
|----------------------|-------|-----|-----|----|----|----|-----|------|--------------------|
| | I | II | III | IV | V | VI | VII | VIII | |
| Particle size | 0 | 2 | 10 | 20 | 38 | 45 | 53 | 60 | μm |
| Stirring speed | 450 | 500 | | | | | | | rpm |
| Stirring temperature | 620 | 650 | | | | | | | $^{\circ}\text{C}$ |

Table 4 Plan of full factorial experiments

| Std order | Run order | Factor 1 | Factor 2 | Factor 3 |
|-----------|-----------|------------------------------------|-------------------------|--|
| | | A: Particle size (μm) | B: Stirring speed (rpm) | C: Stirring temperature ($^{\circ}\text{C}$) |
| 9 | 1 | 20 | 500 | 620 |
| 16 | 2 | 38 | 450 | 650 |
| 12 | 3 | 20 | 450 | 650 |
| 8 | 4 | 10 | 450 | 650 |
| 5 | 5 | 10 | 500 | 620 |
| 3 | 6 | 2 | 450 | 620 |
| 17 | 7 | 45 | 500 | 620 |
| 11 | 8 | 20 | 450 | 620 |
| 2 | 9 | 2 | 500 | 650 |
| 10 | 10 | 20 | 500 | 650 |
| 6 | 11 | 10 | 500 | 650 |
| 21 | 12 | 53 | 500 | 620 |
| 1 | 13 | 2 | 500 | 620 |
| 24 | 14 | 53 | 450 | 650 |
| 13 | 15 | 38 | 500 | 620 |
| 23 | 16 | 53 | 450 | 620 |
| 4 | 17 | 2 | 450 | 650 |
| 22 | 18 | 53 | 500 | 650 |
| 14 | 19 | 38 | 500 | 650 |
| 18 | 20 | 45 | 500 | 650 |
| 19 | 21 | 45 | 450 | 620 |
| 20 | 22 | 45 | 450 | 650 |
| 15 | 23 | 38 | 450 | 620 |
| 7 | 24 | 10 | 450 | 620 |

caused that the experimental density values have been lower than that of theoretical density values (Punith *et al.* 2015, Kim *et al.* 1992).

The results taken from study showed that when the solidification-cooling rate is decreased, the crystalline grain size of the matrix alloy and eutectic silicon phase are increased and on the other hand the tensile and bending strength and hardness are decreased. Fracture surfaces of the MMCs broken and cleaved $\text{Al}_2\text{O}_3/\text{SiC}$ particles were observed on the fracture surface of composites (Zhu and Liu 1993, Kennedy and Wyatt 2000).

3. General full factorial design

General full factorial design method is chosen for the design of mechanical testing of composite materials. Experiments are planned by varying particle size, stirring speed and stirring temperature. All levels of each factor are chosen for the study. Particle size levels are 2, 10, 20, 38, 45, 53 and 60 μm , stirring speed levels are 450 and 500 rpm, stirring temperature levels are 620°C and 650°C. The levels selected for each factor in the design are shown in Table 3. The Minitab16.0 software package (Minitab, Inc., State College, PA) is used for designing the experiments. The plan of experiments is prepared by randomizing the experiments in order to avoid the accumulation of errors. The experiments are conducted based on the randomized run order as given in Table 4.

Test results were subjected to the analysis of variance (ANOVA). Besides, a multiple linear regression Eq. (1) for these experiments can be drawn as

$$Y = a_0 + a_1x_1 + a_2x_2 + a_3x_3 + a_4x_4 + a_5x_1x_2 + a_6x_1x_3 \dots \quad (1)$$

a_0 is the response variable at base level and $a_1, a_2, a_3, a_4, a_5, a_6, a_7, a_8, a_9$ and a_{10} are coefficients associated to each variable or interaction coefficient. Y refers the tensile strength and bending strength of the composite material.

4. Results and discussion

4.1 Statistical analysis of variance (ANOVA)

Table 5-6 shows the results of the analysis of variance (ANOVA) table with the average the tensile strength and bending strength values. ANOVA table shows source, degree of freedom (DF), sequential sum of squares ($Seq\ SS$), adjusted means squares ($Adj\ MS$), F value and percentage of contribution ($C\%$). In this study, only double interactions are investigated for all responses and level of confidence is chosen as 95%. The last column of the table shows the percentage of contribution, C (%), of each factor on the total variation indicating the degree of influence on the result. The percentage of contribution is calculated using the following formula Eq. (2) (Patel and Patel 2012, Pai *et al.* 2010).

$$C (\%) = \frac{Seq\ SS_F}{Seq\ SS_T} \times 100 \quad (2)$$

where $Seq\ SS_F$ is the sum of squares of the factors or the interactions and $Seq\ SS_T$ is total sum of squares. The factors and the interactions that have bigger F value than $F_\alpha = 5\%$ and bigger C (%)

Table 5 Analysis of variance (ANOVA) for the tensile strength

| Source | DF | Seq SS | Adj MS | F | P | C (%) |
|--|----|---------|---------|--------|-------|-------|
| Particle size (μm) | 5 | 7248.73 | 1449.75 | 315.75 | 0 | 99.4 |
| Stirring speed (rpm) | 1 | 0.18 | 0.18 | 0.04 | 0.849 | 0.002 |
| Stirring temperature ($^{\circ}\text{C}$) | 1 | 1.35 | 1.35 | 0.29 | 0.610 | 0.019 |
| Particle size (μm) \times Stirring speed (rpm) | 5 | 5.03 | 1.01 | 0.22 | 0.939 | 0.069 |
| Particle size (μm) \times Stirring temperature ($^{\circ}\text{C}$) | 5 | 6.74 | 1.35 | 0.29 | 0.898 | 0.092 |
| Stirring speed (rpm) \times Stirring temperature ($^{\circ}\text{C}$) | 1 | 6.51 | 6.51 | 1.42 | 0.287 | 0.089 |
| Error | 5 | 22.96 | 4.59 | | | 0.315 |
| Total | 23 | 7291.52 | | | | |

* S = 2.14276; R-Sq = 99.69%; R-Sq (adj) = 98.55%

Notes: *DF*, Degrees of freedom; *Seq SS*, Sequential sum of squares; *Adj SS*, Adjusted sum of squares; *Adj MS*, Adjusted means squares. *C*, Percentage of contribution

value than the *C* (%) value of the error associated are taken as statistically and physically significant factors and interactions (Patel *et al.* 2013, Toptan *et al.* 2012).

Analysis of variance (ANOVA) technique is used to check the adequacy of the developed empirical relationship. In this investigation, the desired level of confidence is considered to be 99%. The model *F* value of 315.77 implies that the model is significant. There is only a 0.015% chance that a model *F* value this large could occur due to noise.

It is observed from the ANOVA table for the tensile strength (Table 5) that the *P* value of the particle size is zero. This indicates that the above mentioned factors are the major influential factors on the tensile strength. However, the *P* values of stirring speed, stirring temperature factor and interactions between the particle size and stirring speed, particle size and stirring temperature, stirring speed and stirring temperature are observed to be 0.849, 0.610, 0.939, 0.898 and 0.287 respectively, indicating insignificant interactions.

The goodness of fit of the model is checked by the determination coefficient (R^2). The coefficient of determination (R^2) is calculated to be 0.8768 for response. This implies that 76.50% of experimental data confirms the compatibility with the data predicted by the model, and the model does not explain only 0.034% of the total variations. The R^2 value is always between 0 and 1, and its value indicates correctness of the model. For a good statistical model, R^2 value should be close to 1.0.

The adjusted R^2 value reconstructs the expression with the significant terms each predicted value matches its experimental value well as shown in Table 5. The value of the adjusted determination coefficient ($\text{Adj } R^2 = 0.73$) is also high to advocate for a high significance of the model. The $\text{Pred } R^2$ is 0.6497 that implies that the model could explain 95% of the variability in predicting new observations. This is in reasonable agreement with the $\text{Adj } R^2$ of 0.73. The value of coefficient of variation is also low as 0.034 indicates that the deviations between experimental and predicted values are low. Adeq precision measures the signal to noise ratio. (Dwivedi *et al.* 2012) have been presented similar results.

It is observed from the ANOVA Table 6 for the bending strength that the *P* value of the particle size, stirring speed and stirring temperature are zero. This indicates that the above mentioned factors are the major influential factors on the bending strength. However, the *P* values of interactions among the particle size and stirring speed, particle size and stirring temperature,

Table 6 Analysis of variance (ANOVA) for bending strength

| Source | DF | Seq SS | Adj MS | F | P | C (%) |
|--|----|----------|---------|----------|-------|-------|
| Particle size (μm) | 5 | 12182.12 | 2436.42 | 19701.54 | 0 | 99.41 |
| Stirring speed (rpm) | 1 | 13.50 | 13.50 | 109.16 | 0 | 0.11 |
| Stirring temperature ($^{\circ}\text{C}$) | 1 | 57.04 | 57.04 | 461.25 | 0 | 0.47 |
| Particle size (μm) \times Stirring speed (rpm) | 5 | 0.38 | 0.08 | 0.61 | 0.697 | 0.00 |
| Particle size (μm) \times Stirring temperature ($^{\circ}\text{C}$) | 5 | 1.12 | 0.22 | 1.81 | 0.266 | 0.01 |
| Stirring speed (rpm) \times Stirring temperature ($^{\circ}\text{C}$) | 1 | 0.20 | 0.20 | 1.63 | 0.258 | 0.00 |
| Error | 5 | 0.62 | 0.12 | | | |
| Total | 23 | 12254.98 | | | | |

* $S = 0.351663$; $R\text{-Sq} = 99.99\%$; $R\text{-Sq (adj)} = 99.98\%$

Notes: *DF*, Degrees of freedom; *Seq SS*, Sequential sum of squares; *Adj SS*, Adjusted sum of squares; *Adj MS*, Adjusted means squares. *C*, Percentage of contribution

stirring speed and stirring temperature are observed to be 0.697, 0.266, 0.258 respectively, indicating insignificant interactions.

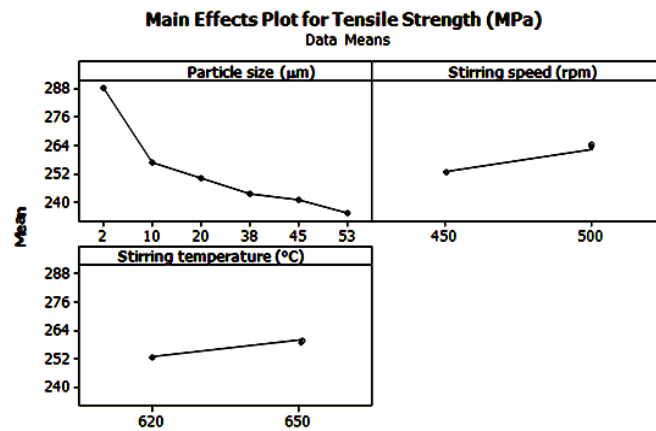
The adjusted R^2 value reconstructs the expression with the significant terms each predicted value matches its experimental value well as shown in Table 6. The value of the adjusted determination coefficient ($\text{Adj } R^2 = 0.8935$) is also high to advocate for a high significance of the model. The $\text{Pred } R^2$ is 0.8699 that implies that the model could explain 95% of the variability in predicting new observations. This is in reasonable agreement with the $\text{Adj } R^2$ of 0.8935. The value of coefficient of variation is also low as 0.0264 indicates that the deviations between experimental and predicted values are low. Adeq precision measures the signal to noise ratio. (Dwivedi *et al.* 2012) have been presented similar results.

4.2 Analysis of factors on the tensile strength and bending strength

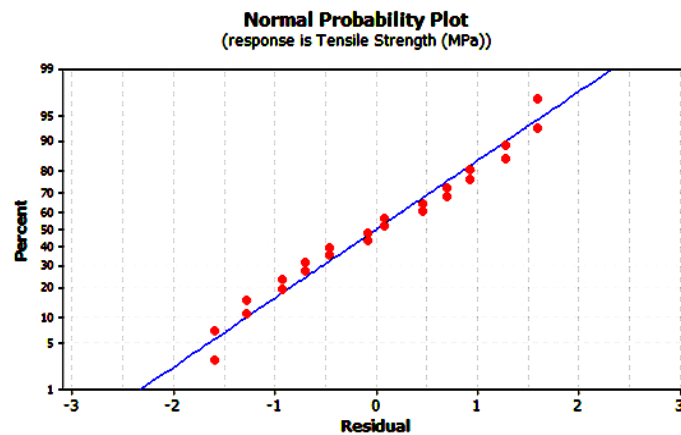
The influence of each control factor (particle size, stirring speed, and stirring temperature) on the tensile strength is analysed with a main effects plot. The optimum values of these control factors could be easily evaluated from this graph. Fig. 5(a) shows the main effect plots for the tensile strength values. The tensile strengths values decreased with particle size and stirring temperature, increased with stirring speed. Normal probability plot of the tensile strength values of composite specimens is shown in Fig. 5(b). As can be seen on the graph, the values are reasonably fitted to normal distribution. Similar results are also reported (Soon *et al.* 1995, Devaraju *et al.* 2013a, b, Rajmohan *et al.* 2013).

The influence of each control factor (particle size, stirring speed, and stirring temperature) on the bending strength was analysed with a main effects plot. The optimum values of these control factors could be easily evaluated from this graph. Fig. 6(a) shows the main effect plots for bending strength values. The bending strength values decreased with particle size and stirring temperature, increased with stirring speed. Normal probability plot of bending strength values of composite specimens is shown in Fig. 6(b). As can be seen on the graph, the values are reasonably fitted to normal distribution. This result is similar to that reported by (Fukumoto and Rajmohan *et al.* 2006).

The plots for particle size, stirring speed and stirring temperature are shown in Figs. 5 and 6. The optimal levels for each control factor can be easily determined from these graphs by



(a) Main effect

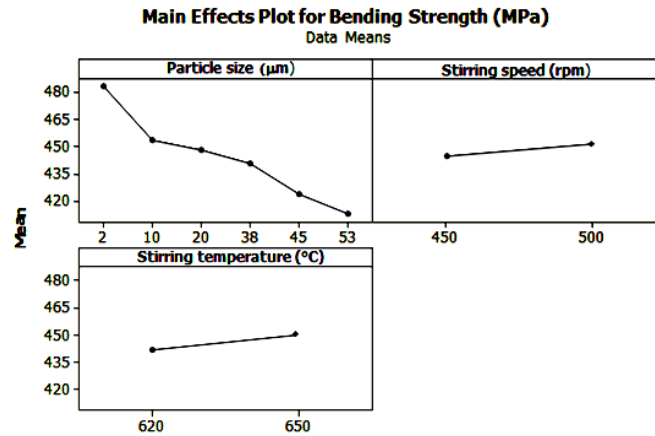


(b) Normal probability

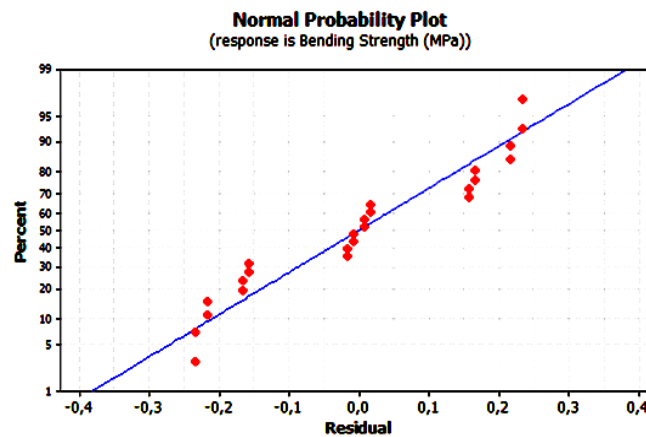
Fig. 5 Plots for the tensile strength of hybrid composites

considering the largest points in accordance with Taguchi's "larger is better" performance characteristic. In the light of Figs. 5 and 6, the factors, namely stirring speed and stirring temperature increase, and they have positive effects on porosity values, hardness, the tensile strength, and bending strength properties of the composite materials. At the same time, with decrease particle sizes on these properties have positive effects. And density values decrease with decrease particle size. Response graphs show the variation of particle size, stirring speed and stirring temperature when the setting of the control factors is changed from one level to another. Figs. 5 and 6 suggest that the optimum conditions for the maximum porosity values, hardness, the tensile strength, and bending strength are the combination of with decrease particle size and with increase stirring speed and stirring temperature of the respective control factors.

Because maximum the tensile strength is obtained for the sample MMC at 2 μm particle size, 500 rpm stirring speed and 650 $^{\circ}C$ stirring temperature for 287.1 MPa and bending strength at 2 μm for 481.2 MPa, the other lower particle size, high stirring speed and stirring temperature are carried out only for the sample MMC. This value is quite high compared with unreinforced Al-Si alloy. When all figures and tables are examined, it can be seen that there is a relation between the



(a) Main effect



(b) Normal probability

Fig. 6 Plots for bending strength of hybrid composites

mechanical properties and particle size and stirring speed and stirring temperature. The increase in stirring speed and stirring temperature increases the wettability by decreasing viscosity. Because of porous formation within the collected $\text{Al}_2\text{O}_3/\text{SiC}$ particles and the porousness in matrix, the composites compactness values diminished (Salvador *et al.* 2003). Since particle size diminishes and number of particles in a unit bulk rises, diminishes on the particle size hardness resistance, the tensile strength and bending strength of MMCs have become larger.

4.3 Construction of the mechanical and physical properties maps

Variations of the tensile strength and bending strength of dual ceramic particles ($\text{Al}_2\text{O}_3/\text{SiCp}$) reinforced aluminium matrix composites with the different test conditions are plotted as the mechanical properties maps as shown in Figs. 7-10.

Fig. 7 demonstrates that at the highest hardness values and at the lowest density values a maximum the tensile strength is experienced and the tensile strength gradually increases as the

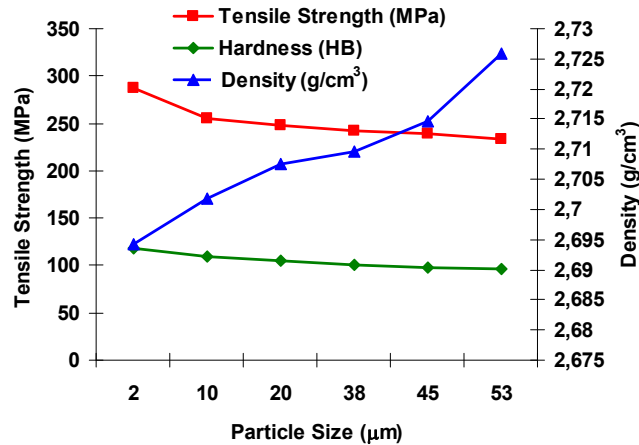


Fig. 7 The tensile strength map of hybrid composite for varying hardness and density values

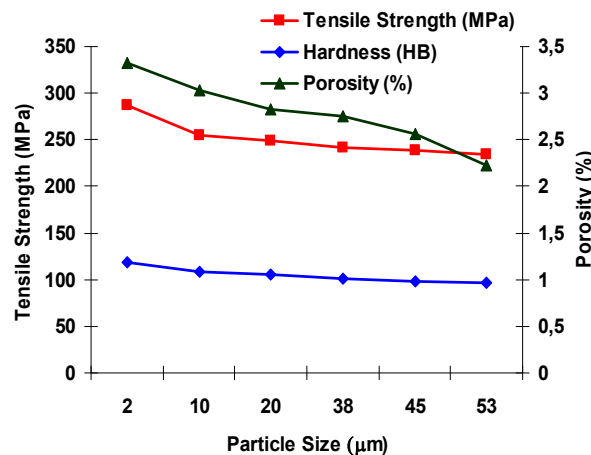


Fig. 8 The tensile strength map of hybrid composite for varying particle sizes and porosity

hardness increases and the density values decreases. It is found that the maximum the tensile strength occurred 287.1 MPa and at a density values of 2.72 gr/cm^3 . Similar results are also reported (Soon *et al.* 1995, Rajmohan *et al.* 2006, Salvador *et al.* 2003).

The Fig. 8 showing the variation of the tensile strength as a function of different test parameters is plotted. It is found from Fig. 8 that, for hybrid composites, the tensile strength decreases as particle size increases from 2 μm to 60 μm and porosity decreases from 3.5 to 2.5%. Similar results are also reported (Devaraju *et al.* 2013a/b, Yilmaz and Buytoz 2001, Alpas and Zhang 1994).

Fig. 9 demonstrates that at the highest hardness and at the lowest density values a maximum bending strength is experienced and the bending strength gradually increases as the hardness increases and the density values decreases. It is found that the maximum bending strength occurred 481.2 MPa and at a density values of 2.72 gr/cm^3 . Similar results are also reported (Alpas and Zhang 1994, Bensam *et al.* 2012).

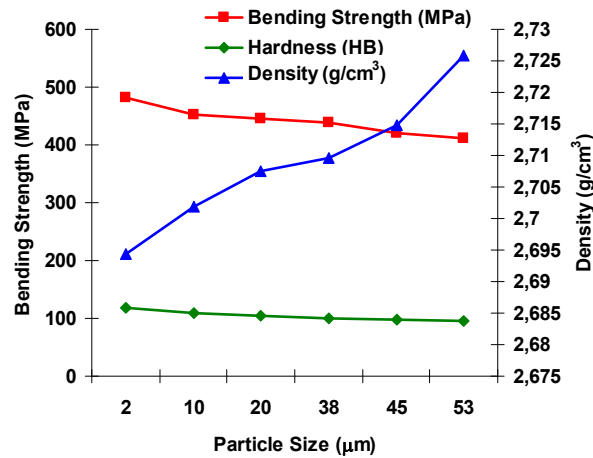


Fig. 9 Bending strength map of hybrid composite for varying hardness and density values

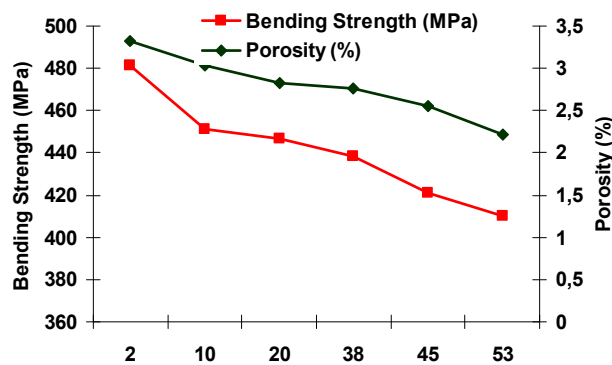


Fig. 10 Bending strength map of hybrid composite for varying particle sizes and porosity

The Fig. 10 showing the variation of bending strength as a function of different test parameters is plotted. It is found from Fig. 10 that, for hybrid composites, the bending strength decreases as particle size increases from 2 µm to 60 µm and porosity decreases from 3.5 to 2.5%. Similar results are also reported (Chu and Wu 1999).

Furthermore, although the hybrid particle size was some effect on the bending and the tensile strength, the fine particle size was a greater effect. The mechanical properties of the fine particle size MMCs were higher than that of the coarse particle size MMCs. Similar coefficients of the mechanical tests results were reported for MMCs by (Wang *et al.* 2010).

4.4 Linear regression model

According to the results above, regression equation based on significant parameters can be determined as follows:

Regression Eq. (3)

$$Y_{\text{Tensile Strength}} = 283.868 - 0.819237 * \text{Particle size} + 0.0035 * \text{Stirring speed} - 0.0158333 * \text{Stirring temperature}$$

$$R^2 = 0.76 \quad (3)$$

Regression Eq. (4)

$$Y_{\text{Bending Strength}} = 517.058 + 1.13998 * \text{Particle size} - 0.0699352 * \text{Stirring speed} - 0.113555 * \text{Stirring temperature}$$

$$R^2 = 0.89 \quad (4)$$

In multiple linear regression analysis, R^2 is value of the correlation coefficient and should be between 0.7 and 1. In this study, regression models are obtained from the mechanical measurements for the tensile strength matched very well with the experimental data ($R^2 = 0.76$) and for bending strength matched very well with the experimental data ($R^2 = 0.89$).

5. Conclusions

The Taguchi method was applied to investigate the effects of particle size, stirring speed and stirring temperature on the mechanical properties and physical behaviour of hybrid Al₂O₃/SiC reinforced aluminium-matrix composites. The conclusions drawn from the study can be summarized as follows:

- A multiple linear regression model has been used to derive an empirical relationship between particle size (PS), stirring speed (SS), and stirring temperature (ST) in the following form: The tensile strength = $283.868 - 0.819237 * \text{Particle size} + 0.0035 * \text{Stirring speed} - 0.0158333 * \text{Stirring temperature}$ and Bending Strength = $517.058 + 1.13998 * \text{Particle size} - 0.0699352 * \text{Stirring speed} - 0.113555 * \text{Stirring temperature}$
- An R^2 value of 0.76 obtained for the tensile strength and R^2 value of 0.89 for bending strength, which indicates reasonable accuracy of the empirical equation to take into account all the variations of parameters with minimal error value
- The validation test results show that the experimental values were within the calculated confidence interval for a significance level of 95% confidence level
- Taguchi's orthogonal design was developed to predict the quality characteristics (the tensile strengths and bending strength) within the selected range of process parameters (particle size, stirring speed and stirring temperature). The results were validated through ANOVA

References

- Alpas, A.T. and Zhang, J. (1994), "Effect of microstructure (particulate size and volume fraction) and counterface material on the sliding wear resistance of particulate-reinforced aluminium matrix composites", *Metal. Mater. Trans. A*, **25**(5), 969-983.
- Anand, K., Mahapatra, M.M. and Jha, P.K. (2013), "Modelling the abrasive wear characteristics of in-situ synthesized Al-4.5%Cu/TiC composites", *Wear*, **306**(1-2), 170-178.
- Azmah, H.M.A., Chang, C.S. and Khang, C.O. (2011), "Effect of a two-step solution heat treatment on the microstructure and mechanical properties of 332 aluminium silicon cast alloy", *Mater. Des.*, **32**(4), 2334-2338.
- Bensam, R., Marimuthu, P., Prabhakar, M. and Anandkrishnan, V. (2012), "Effect of sintering temperature and time intervals on workability behaviour of Al-SiC matrix P/M composite", *Int. J. Adv. Manufact.*

- Techn.*, **61**(1), 237-252.
- Caracostas, C.A., Chiou, W.A., Fine, M.E. and Cheng, H.S. (1997), "Tribological properties of aluminium alloy matrix TiB₂ composite prepared by *in-situ* processing", *Metal. Mater. Trans. A*, **28**(2), 491-502.
- Carmita, C.N. (2013), "Optimization of cutting parameters for minimizing energy consumption in turning of AISI 6061 T6 using taguchi methodology and ANOVA", *J. Clean. Produc.*, **53**, 195-203.
- Ceschini, L., Minak, G. and Morri, A. (2006), "Tensile and fatigue properties of the AA6061/20 vol.% Al₂O₃p and AA7005/10 vol.% Al₂O₃p composites", *Comp. Sci. Tech.*, **66**(2), 333-342.
- Chou, S.N., Huang, J.L., Lii, D.F. and Lu, H.H. (2006), "Mechanical properties of Al₂O₃/aluminium alloy A356 composite manufactured by squeeze casting", *J. Alloy. Compounds*, **419**(1-2), 98-102.
- Chu, S. and Wu, R. (1999), "The structure and bending properties of squeeze-cast composites of A356 aluminium alloy reinforced with alumina particles", *Comp. Sci. Tech.*, **59**(1), 157-162.
- Devaraju, A., Kumar, A. and Kotiveerachari, B. (2013a), "Influence of rotational speed and reinforcements on wear and mechanical properties of aluminium hybrid composites via friction stir processing", *Mater. Des.*, **45**, 576-585.
- Devaraju, A., Kumar, A., Kumaraswamy, A. and Kotiveerachari, B. (2013b), "Influence of reinforcements (SiC and Al₂O₃) and rotational speed on wear and mechanical properties of aluminium alloy 6061-T6 based surface hybrid composites produced via friction stir processing", *Mater. Des.*, 2013, **51**, 331-341.
- Dwivedi, S.P., Kumar, S. and Kumar, A. (2012), "Effect of turning parameters on surface roughness of A356/5%SiCp composite produced by electromagnetic stir casting", *J. Mech. Sci. Tech.*, **26**(12), 3973-3979.
- Elayaperumal, R. and Issac, F. (2013), "A statistical analysis of optimization of wear behaviour of Al-Al₂O₃ composites using taguchi technique", *Proc. Eng.*, **64**, 973-982.
- Ezatpour, H.R., Sajjadi, S.A., Sabzevar, M.H. and Huang, Y. (2014), "Investigation of microstructure and mechanical properties of Al6061-nanocomposite fabricated by stir casting", *Mater. Des.*, **55**, 921-928.
- Fisher R.A. (1961), *Design of Experiments*, Oliver Boyd, Edinburgh, UK.
- Fukumoto, I., Mekar, S., Shibata, S. and Nakayama, K. (2006), "Fabrication of composite material using alumina agglomerated sludge and aluminium powder by spark plasma sintering", *Int. J. Ser Solid Mech. Mater. Eng.*, **49**(1), 91-94.
- Gopalakrishnan, S. and Murugan, N. (2012), "Production and wear characterization of AA 6061 matrix titanium carbide particulate reinforced composite by enhanced stir casting method", *Comp. Part B: Eng.*, **43**(2), 302-308.
- Gui, M.C., Wang, D.B., Wu, J.J., Yuan, G.J. and Li, C.G. (2000), "Microstructure and mechanical properties of cast (Al-Si)/SiCp composites produced by liquid and semisolid double stirring process", *Mater. Sci. Tech.*, **16**(5), 556-563.
- Gupta, M., Ibrahim, I.A., Mohamed, F.A. and Lavernia, E.J. (1991), "Wetting and interfacial reactions in Al-Li-SiC_p metal matrix composites processed by spray atomization and deposition", *J. Mater. Sci.*, **26**(24), 6673-6684.
- Han, N.L., Wang, Z.G. and Sun, L.Z. (1995), "Low cycle fatigue behaviour of SiCp reinforced aluminium matrix composite at ambient and elevated temperature", *Scr. Metal. Mater.*, **32**(11), 1739-1745.
- Hashim, J., Looney, L. and Hashmi, M.S.J. (1999), "Metal matrix composites: production by the stir casting method", *J. Mater. Proc. Tech.*, **92-93**, 1-7.
- Hashim, J., Looney, L. and Hashmi, M.S.J. (2002), "Particle distribution in cast metal matrix composites", *J. Mater. Proc. Tech.*, **123**(2), 251-257.
- Kennedy, A.R. and Wyatt, S.M. (2000), "The effect of processing on mechanical properties and interfacial strength of aluminium/TiC MMCs", *Comp. Sci. Tech.*, **60**(2), 307-314.
- Kim, Y.H., Lee, C.S. and Han, K.S. (1992), "Fabrication and mechanical properties of aluminium matrix composite materials", *J. Compos. Mater.*, **26**, 1062-1086.
- Kok, M. (2005), "Production and mechanical properties of Al₂O₃ particle-reinforced 2024 aluminum alloy composites", *J. Mater. Proc. Tech.*, **161**(3), 7-381.
- Kong, H.B., Jien, L.S. and Ten, J.M. (1996), "The Interfacial compounds and SEM fractography of squeeze-cast SiCp /6061 Al composites", *Mater. Sci. Eng. A*, **206**(1), 110-119.

- Lloyd, D.J. and Brotzen, F.R. (1999), "Particle reinforced aluminium and mg matrix composites", *Int. Mater. Reviews*, **39**(1), 1-39.
- Naher, S., Brabazon, D. and Looney, L. (2003), "Simulation of the stir casting process", *J. Mater. Proc. Tech.*, **143-144**, 567-571.
- Pai, D., Rao, S., Shetty, R. and Nayak, R. (2010), "Application of response surface methodology on surface roughness in grinding of aerospace materials (6061Al-15Vol% SiC25p)", *ARPN J. Eng. App. Sci.*, **5**(6), 23-28.
- Patel, R.R. and Patel, V.A. (2012), "Effect of machining parameters on Surface roughness and power consumption for 6063 Al alloy TiC Composites (MMCs)", *Int. J. Eng. Res. App.*, **2**(4), 295-300.
- Patel, P.R., Patel, B.B. and Patel, V.A. (2013), "Effect of machining parameters on surface roughness for Al-TiC (5&10%) metal matrix composite using RSM", *Int. J. Res. Eng. Tech.*, **2**(1), 65-71.
- Peters, P.W.M., Hemptenmacher, J. and Schurmann, H. (2010), "The fibre/matrix interface and its influence on mechanical and physical properties of Cu-MMC", *Comp. Sci. Tech.*, **70**(9), 1321-1329.
- Prabu, S.B., Karunamoorthy, L., Kathiresan, S. and Mohan, B. (2006), "Influence of stirring speed and stirring time on distribution of particles in cast metal matrix composite", *J. Mater. Proc. Tech.*, **171**(2), 268-273.
- Punith, G.K., Prakash, J.N., Gowda, S. and Satish, B.B. (2015), "Effect of Particulate Reinforcement on the Mechanical Properties of Al2024-WC MMCs", *J. Miner. Mater. Character. Eng.*, **3**(6), 469-476.
- Radhika, N., Subramanian, R. and Venkat, P.S. (2011), "Tribological behaviour of aluminium/ alumina/graphite hybrid metal matrix composites taguchi's techniques", *J. Miner. Mater. Character. Eng.*, **10**(5), 427- 443.
- Rajmohan, T., Palanikumar, K. and Ranganathan, S. (2013), "Evaluation of mechanical and wear properties of hybrid aluminium matrix composites", *Trans. Nonfer. Metal. Soc. China*, **23**(9), 2509-2517.
- Rajmohan, T., Palanikumar, K. and Arumugam, S. (2014), "Synthesis and characterization of sintered hybrid aluminium matrix composites reinforced with nanocopper oxide particles and micro silicon carbide particles", *Comp., Part B*, **59**, 43-49.
- Ross, P.J. (1996), *Taguchi Techniques for Quality Engineering*, (2nd Edition), McGraw-Hill, New York, NY, USA.
- Roy, R.K. (2001), *Design of Experiments using the Taguchi Approach: 16 Steps to Product and Process Improvement*, John Wiley & Sons, Inc., New York, NY, USA.
- Sajjadi, S.A., Parizi, M.T., Ezatpour, H.R. and Sedghi, A. (2012), "Fabrication of A356 composites reinforced with micro and nano Al₂O₃ particles by a developed compocasting method and study of their properties", *J. Alloys Compound.*, **511**(1), 226-231.
- Salvador, M.D., Amigó, V., Martinez, N. and Busquets, D.J. (2003), "Microstructure and mechanical behaviour of Al-Si-Mg alloys reinforced with Ti-Al inter metallics", *J. Mater. Proc. Tech.*, **143-144**, 605-611.
- Sato, A. and Mehrabian, R. (1976), "Aluminium matrix composites: Fabrication and properties", *Metall. Mater. Trans. B*, **7**(3), 443.
- Soon, H., Chung, H. and Kyung, H. (1995), "The effects of processing parameters on mechanical properties of SiC_w/2124Al composites", *J. Mater. Proc. Tech.*, **48**(1-4), 349-355.
- Srivatsan, T.S. (1996), "Microstructure, the tensile properties and fracture behaviour of Al₂O₃ particulate reinforced aluminium alloy metal matrix composites", *J. Mater. Sci.*, **31**(5), 1375-1388.
- Swamy, A., Ramesha, A., Kumar, G. and Prakash, J. (2011), "Effect of particulate reinforcements on mechanical properties of Al6061-WC and Al6061-Gr MMCs", *J. Miner. Mater. Character. Eng.*, **10**(12), 1141-1152.
- Toptan, F., Kerti, I. and Rocha, L.A. (2012), "Reciprocal dry sliding wear behaviour of B₄Cp reinforced aluminium alloy matrix composites", *Wear*, **290-291**, 74-85.
- Trezona, R.I., Pickles, M.J. and Hutchings, I.M. (2000), "A full factorial investigation of the erosion durability of automotive clear coats", *Trib. Inter.*, **33**(8), 559-571.
- Wang, Y.Q., Afsar, A.M., Jang, J.H., Han, K.S. and Song, J.L. (2010), "Room temperature dry and lubricant wear behaviours of Al₂O₃f/SiCp/Al hybrid metal matrix composites", *Wear*, **268**(7-8), 863-870.

- Yılmaz, O. and Buytoz, S. (2001), "Abrasive wear of Al₂O₃-reinforced aluminium-based MMCs", *Comp. Sci. Tech.*, **61**(16), 2381-2392.
- Zhu, H.X. and Liu, S.K. (1993), "Mechanical properties of squeeze cast zinc alloy matrix composites containing alpha-alumina fibers", *Comp.*, **24**(6), 437.

CC

Nomenclature

| | |
|--------------------------------------|--|
| MMCs | metal matrix composites |
| Al ₂ O ₃ /SiCp | alumina/silicon carbide particle |
| A332 | aluminium code |
| μm | micron meter |
| ρ_m | matrix density values |
| ρ_{th} | theoretical density values |
| EDS | energy dispersive spectroscopy |
| SEM | scanning electron microscope |
| HB | hardness brinell |
| MPa | mega pascal |
| rpm | revolution per minute |
| DOE | design of experiment |
| S/N ratio | signal-to-noise ratio |
| Y | refers (the tensile strength and bending strength) |
| ANOVA | analysis of variance |
| <i>DF</i> | degree of freedom |
| <i>Seq SS</i> | degree of freedom |
| <i>Adj MS</i> | adjusted means squares |
| F | fisher's values |
| P | level of significance |
| C % | percentage of contribution |
| <i>Seq SS_F</i> | sum of squares |
| <i>Seq SS_T</i> | total sum of squares |
| <i>DF</i> | degrees of freedom |
| <i>R-Sq</i> | sum of squares |
| <i>R-Sq(Adj)</i> | adjusted sum of squares |
| <i>Seq SS</i> | sequential sum of squares |
| <i>Adj SS</i> | adjusted sum of squares |
| <i>Adj MS</i> | adjusted means squares |
| <i>R²</i> | regression analysis |
| <i>PS</i> | particle size |
| <i>SS</i> | stirring speed |
| <i>ST</i> | stirring temperature |